Asymmetric Effect on the Length Dependence of Oligo-(Phenyleneethynylene) Based Molecular Junctions

Yinqi Fan,[a,b] Sylvain Pitie,[c] Chenguang Liu,[a] Cezhou Zhao,[d] Chun Zhao,[d] Mahamadou Seydou,[c] Yannick J. Dappe,[e] Richard J. Nichols [b] and Li Yang*[a,b]

a. Department of Chemistry, Xi'an-Jiaotong Liverpool University, Suzhou, 215123, China.

b. Department of Chemistry, University of Liverpool, Liverpool, L69 7ZD, UK.

c. Université de Paris, ITODYS, CNRS, F-75006 Paris, France.

d. Department of Electrical and Electronic Engineering, Xi'an-Jiaotong Liverpool University, Suzhou, 215123, China.

e. SPEC, CEA, CNRS, Université Paris-Saclay, CEA Saclay 91191 Gif-sur-Yvette Cedex, France.

KEYWORDS. Single molecular electronics, graphene contacts, oligo (phenylene ethynylene)s, density functional theory.

Corresponding Author

li.yang@xjtlu.edu.cn

Abstract:

It is well known that the electrical conductance of molecular junctions in the tunneling regime varies exponentially with the length of the molecular backbone. This behavior is strongly influenced by the anchoring groups, which connect the molecular backbone to the electrodes and locate the HOMO and LUMO resonances with respect to the Fermi level. Nevertheless, most of the studies have been performed on symmetric junctions, namely using the same electrodes and anchoring groups at both sides of the junctions. There have only recently been some reports detailing the influence of introducing asymmetry into single molecular junctions, by using different contacts or different anchoring groups at either end of the molecular bridge. These studies have revealed that such junction asymmetry impacts strongly on the electrical characteristics. In this study, Au and graphene electrodes were used to provide the asymmetry to a single molecular junction. The conductance and length dependence of amine and methyl sulfide terminated oligo-(phenylene ethynylene) have been determined experimentally and theoretically. The impact of introducing this asymmetric has been quantified by comparing the conductance and β values of OPE based molecules within Au/Au electrode and Au/graphene junctions, respectively. Our results show that the introduction of a graphene electrode leads to lower conductance values and attenuation factors, similarly to what has been previously observed in alkane chains. This is attributed to a shift of the electronic molecular levels toward the Fermi level mainly driven by the acetylene groups linking adjacent phenyl groups.

Introduction

Aviram and Ratner [1] first proposed the creative idea of using molecules as molecular rectifiers and within single molecule circuits in 1974. Since then, many fundamental aspects of molecular electronics have been extensively developed, helped by the development of platforms to reliably electrically contact molecules and methods to theoretically model their transport properties. [2-5] Molecular electronics has even been extended beyond fundamental studies, for example larger area molecular junctions (MJs) have been recently commercially deployed as an active component in audio distortion circuits for guitar pedals [6]. Efficient charge transport across individual molecules and electrode interfaces is essential for many chemical, physical and biological processes. Here fundamental knowledge supplied by single molecule measurements and accompanying theory is of paramount importance for understanding such charge transfer processes.[7-9] Commonly, electron transport in short molecules is characterized by an exponential decrease in conductance with the increasing molecular length. [10-12] This decrease of conductance with length of the single-molecule junction can be quantitatively described by the attenuation factor (β). For molecules following a direct tunneling mechanism, the attenuation factor is associated with the conductance G through the simple equation $G = A\,exp(-\beta L)$, where *A* is the contact resistence and *L* is the molecular length. [13-14] To date, the attenuation factor of single-molecular junctions formed with wide various molecules has been extensively investigated. It is widely accepted that the chemical structure of the molecular bridge strongly affects the attenuation factors. Generally speaking, π-conjugated structures present a smaller HOMO-LUMO gap than saturated organic molecules and thus have a significantly lower attenuation factor.[15-17] For example, fully saturated alkanes were reported to have higher attenuation factors (6-12 nm^{-1}) [18-19] than oligo-phenylene (4.3 nm^{-1}) [20]. Moreover, π-conjugated molecules with non-aromatic systems were reported with lower β values than purely aromatic molecules, such as alkenes (2.2 nm^{-1}) [21] and alkynes (0.6 nm^{-1}) [22]. Many studies also show that the attenuation factor depends on the anchoring groups of the molecules in the MJs. [23-24] The influence of various anchoring groups on junction formation and electrical transport properties has also been established, with anchoring groups investigated including thiol [25], amino [26-27], pyridyl [28-29], carboxylic acid [30-31], dimethyl phosphine [25], methyl sulfide[32] and Isocyanides. [33, 29] However, for the same molecular backbones, different anchoring groups often (but not always) only weakly affects the attenuation factors of the molecular junction. Examples of analysis for the anchoring group influence on the attenuation factor include a study from Park *et al*., where the length dependence of amine, dimethyl phosphine and methyl sulfide terminated alkanes was considered and a small difference in the β value of each MJs was found. [25] This difference was mainly attributed to the alignment between the Fermi level and the frontier orbitals of the molecular backbone. Oligo (phenylene ethynylene) (OPE) attached to gold contacts through Au-C bonds in MJs have been reported to have similar β

values to those of thiol terminated OPEs, although the former displayed higher conductance values. [34] On the other hand, Moreno-García *et al.* found a large variation in β values for a series of functionalized oligoynes with different anchoring groups and gold contacts. [14] Here the experimental attenuation factors were found to range from between 1.7 nm^{-1} for CN anchoring groups to 3.2 nm^{-1} for thiol anchors. The solvent in which the single molecule measurements are performed has also been found to have a marked impact on attenuation factors.[35-36] An example of this is the study of Milan *et al.* who quantified the conductance and attenuation factor of a homologous series of oligoynes. [37] These authors found large differences in attenuations for the oligoyne molecular wires with different organic solvents. This was theoretically explored using DFT-based models of the solvated molecular junction, with the solvent molecules interacting with the molecular junction and influencing the transport properties.

The electrode material is another important factor which influences the electron transport characteristics and the attenuation factor in MJs. Many experiments show that the strength of the electronic coupling between the anchoring group and the electrode affects the electrical conductance and the β value of the molecular junction,[38-39] for instance Au [40], Ag [41], Cu [42], ITO [43], graphite [8], graphene [44]. Obviously, strong coupling and small contact resistance are more beneficial for effective electronic transport across molecular junction. Kim *et al.* found that for both alkane and phenylene, the Au electrode yielded a higher conductance and a higher β value than Ag electrode.[45] Additionally, silver electrodes were reported to have better electrical contact with thiol-terminated silanes when compared to Au and Pt. [41] He *et al.* built metal free MJs by using carbon fiber as a top electrode and graphene as bottom electrode. [46] They suggested that carbon contacted single molecular junctions present a lower β value than Au contacted MJs. Kim *et al.* formed symmetric and non-symmetric MJs through amine terminated oligophenyls with Au/Au ("symmetric") and graphite/Au ("non-symmetric") electrodes.[8] They found that the β values of these two MJs are the same. Similarly, Zhang *et al.* also studied the effect of non-symmetric electrode systems on molecular conductance and β values.[27, 47] They found that the replacement of one of the Au electrodes by a graphene one resulted in a lower conductance at short molecular length but also a lower β value, leading to higher conductance at longer molecular lengths. This phenomenon is explained by the coupling asymmetry between the strong chemisorption of molecules on gold electrodes and the weak van der Waals contacts on graphene. However, Tao *et al.* found the influence of the junction symmetry depends on the decrease of conjugation of the molecular backbone. They found that the junction asymmetry has a greater impact for alkane containing molecular bridges than for phenylene one[43]. These preliminary studies indicate that a full understanding of charge transport properties remains a complicated task for non-symmetric MJs systems, and therefore, further studies of such non-symmetric MJs are likely to reveal new insights which have been less routinely investigated to date.

In the present work, we fabricated OPE based MJs with Au and graphene contacts to give non-symmetric junctions. OPE has been a popular model system in single molecular electronics. [48-49] A feature of the OPE system is its smaller β value when compared to alkane and phenylene molecular bridge, thereby promoting longer range transport within a tunnelling regime. [50-51] Here, we also achieve a reduction of attenuation factors for amine and methyl sulfide terminated OPE based MJs when introducing a non-symmetric Au/graphene electrode contacting. In particular, we explored the effect of electrodes and anchoring group to the charge transport evolution of MJs. Density Functional Theory (DFT) and non-equilibrium Green Function (NEGF) calculations support the experimental results and confirm the impact of junction asymmetry on electronic transport properties for electronically delocalized MJs.

Experimental Section

Materials and conductance measurements

In this study, all the purchased chemicals are directly used without further purification. The compounds used in the single-molecule conductance measurements are shown in Figure 1(a). **1a** and **2a** were purchased from J&K Scientific (99%). **3a**, **2b** and **3b** were synthesized by a Sonogashira cross-coupling reaction. The synthesis of **1b** followed the procedure reported by Joseph *et al.* [52] The details of molecular synthesis can be found in the supporting information. The single-molecule conductance measurements of target molecules were performed using STM- *I(s)* technique developed and describe by Haiss et al. (Figure 1(b)).[53] The gold STM tips were fabricated by the electrochemical etching method reported by Ren et al. in 2004. [54] A gold wire (Tianjing Lucheng Metal) with 0.25 mm diameter and 99.99 % purity was used as the tip material. The etching solution was a mixed solution of hydrochloric acid and ethanol with a volume ratio of 1: 1. During the etching process, a gold ring of about 8 mm in diameter was placed on the surface of the solution. A gold wire was immersed in the center of the ring and an etching voltage of + 2.3 V was applied. The 1×1 cm size gold and graphene substrates were purchased from the Arrandee Gold (Germany) and Graphene Supermarket (USA), respectively. Before the conductance measurements, the target molecules were dissolved in mesitylene (Sigma Aldrich, 99%) to prepare 1 mM solutions. All the measurements were performed under a stable liquid environment. The tip bias and set point currents were set to different values according to which molecule was under study. For example, the tip bias was 100 mV and the current set point was 100 nA for Au/1a/Au MJs. Over 10000 current-distance curves were collected for each molecular junction. Then, all collected curves were processed by a fully automatic sorting program developed by

our group.[55] In this process noisy curves and the direct exponential tunneling curves were firstly screened out. Then, according to the current value of the corresponding plateau, the selected current-distance curves were automatically divided into several groups with the same bin size. The curves of different groups were plotted as one-dimensional (1D) and two-dimensional (2D) conductance histograms to find the dominant conductance value of MJs. In addition, the break-off distances of each molecular junction were calculated through the 2D conductance-distance histograms.

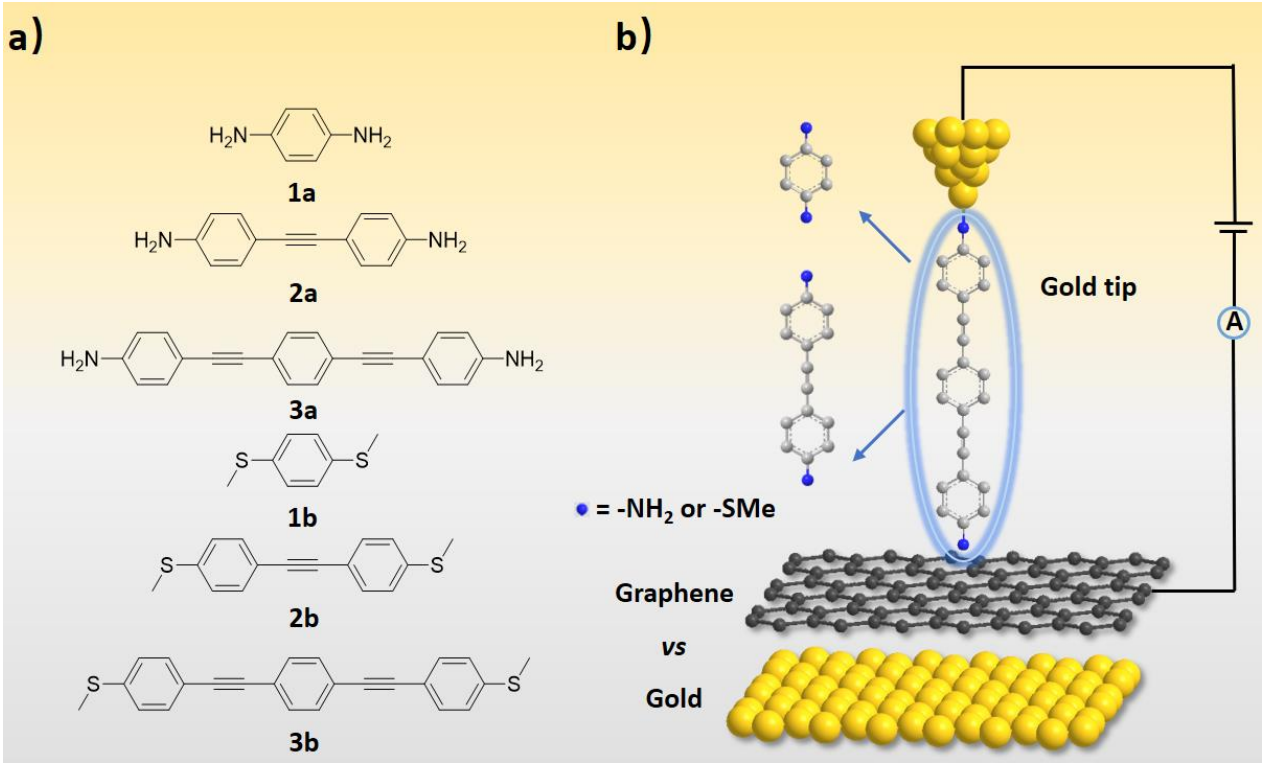

Figure 1. (a) Chemical structure of studied molecules; (b) Schematic illustration of the formation of OPE molecular junction.

Computational details

In order to interpret the experimental results, we have performed Density Functional Theory (DFT) calculations on the different types of model MJs involved in this study. To this end, we have used the very efficient localized-orbital basis sets Fireball code [56]. Numerical orbitals sp^3d^5 have been used to determine the atomic configuration and the electronic properties of the MJs. The corresponding cut-off radii (in atomic units) are s = 4.6, p = 5.2, d = 4.2 (Au), s = 4.1, p = 4.5 (C), s = 4.2, p = 4.2 (N), s = 3.1, p = 3.9 (S), and s = 4.1 (H). This basis set has been used successfully in previous works on MJs [27, 47]. To model the junctions, we have considered the OPE molecule with one, two or three molecular units, sandwiched between the anchoring groups (either amine -NH_2 or methyl sulfide

-SMe) and between gold electrodes (Au tip of 35 atoms) or gold and graphene electrodes (a 5x5 graphene supercell in the XY plane). Then, we have optimized the corresponding geometry until the forces went below 0.1 eV/Å. Also, we have used a non-equilibrium Green Function (NEGF) formalism within a fast Ficher-Lee approach [57] to determine the electronic transmission and the corresponding conductance of the MJs.

Results and Discussions

Conductance of amine terminated OPE molecules

The amine terminated OPE **1a**-**3a** MJs formed using gold electrodes were firstly investigated. Figure 2(a-d) shows the typical conductance traces and the 1D conductance histograms of each MJs. The most probable conductance values were obtained by Gaussian distribution peak fitting. The conductance value of Au/**1a**/Au is around 460 nS. The same molecular junction was also studied by Yoo *et al.* and Zhao *et al.* and a similar conductance value was reported. [45, 58] The conductance values of **2a** and **3a** are found at around 65 nS and 13 nS, respectively, which is in a good agreement with the result reported by Hong *et al*. [14, 59] To illustrate the non-symmetric contacting effect on the MJs, the molecular conductance of amine terminated OPEs was measured using an Au and a graphene electrode. These measurements were made under the same condition as those with Au electrodes at both sides. Typical conductance traces and 1D conductance histogram of **1a**-**3a** with the Au/graphene electrodes are shown in Figure 2(e-h). As shown in Figure 2(f), **1a** with the "non-symmetric" Au/graphene electrode contacting is found to have a similar conductance value as reported by Tao *et al.* (56 nS). [27] Hence, the molecular junction formed by **1a** has a significantly lower conductance when replacing the Au bottom electrode by graphene electrode. The conductance value of **2a** with Au/graphene electrodes is found to be around 26 nS. Similar to the results with **1a**, the introduction of graphene electrode to form Au/**2a**/Au is associated with a reduction of the junction conductance due to a higher contact resistance. Finally, the molecular conductance value of **3a** with Au/graphene contacting is found to be very similar to its Au/Au counterpart. However, both conductance values for these longest OPE compounds in the series are small and same, namely 13 nS.

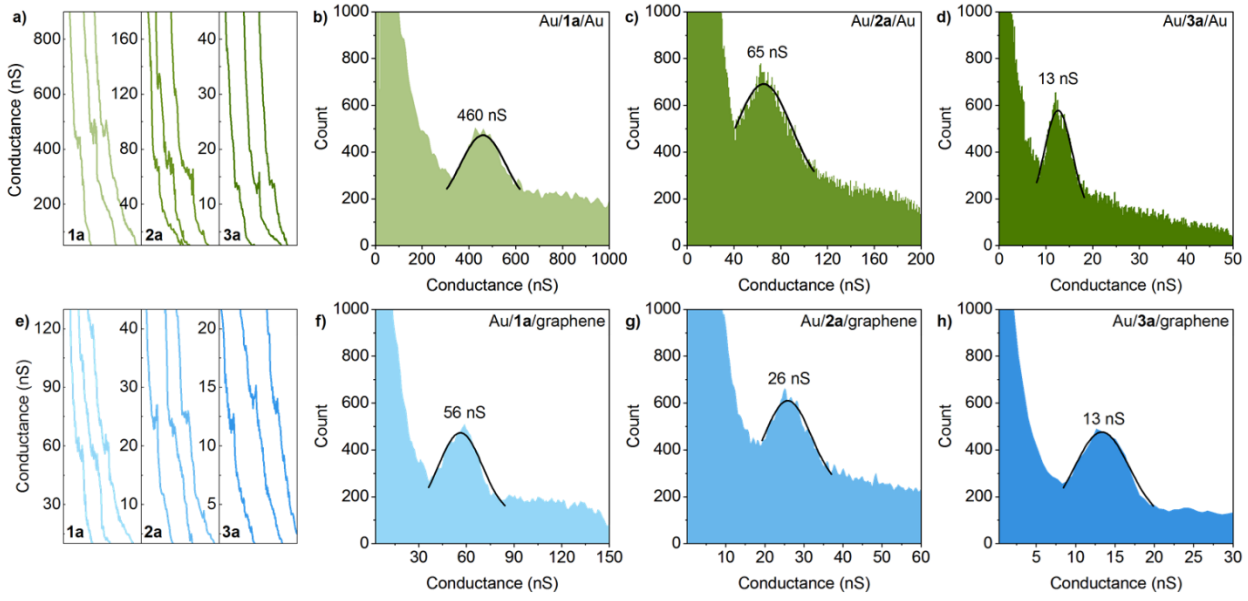

Figure 2. Typical conductance traces of amine terminated OPE molecules (a) with Au/Au electrode; (e) with Au/graphene electrode system. 1D conductance histograms of amine terminated OPE molecules (b-d) with Au/Au electrode; (f-h) with Au/graphene electrode system. The black lines represent the Gaussian distribution peak fitting curves of each MJs.

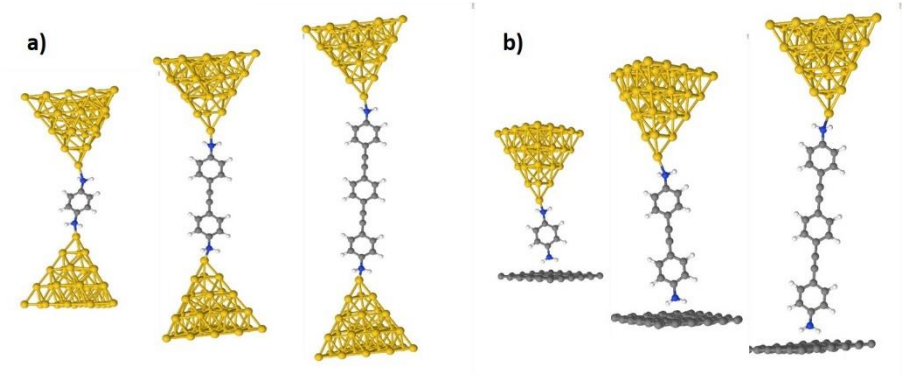

Figure 3. DFT optimized atomic configurations of a) symmetric gold-gold and b) asymmetric gold-graphene amine terminated OPE molecular junctions

These MJs have been studied theoretically using density functional theory. The corresponding optimized geometries for the model MJs are represented in Figure 3. From these configurations, we have determined the corresponding electronic transmission, which is represented in Figure 4(a) for the gold-gold junctions and in Figure 4(b) for the gold-graphene junctions, respectively.

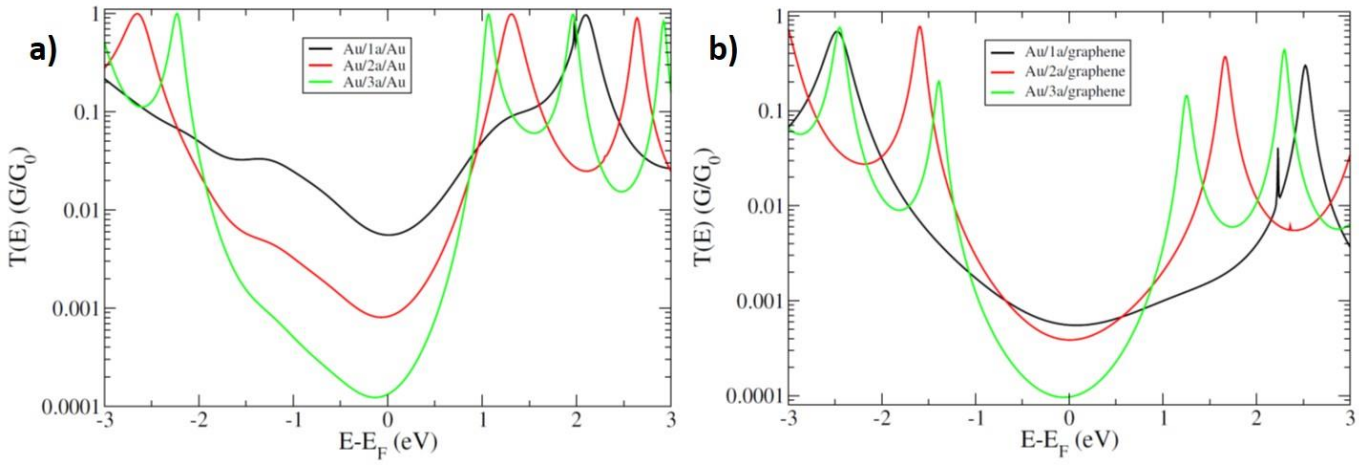

Figure 4. Calculated electronic transmission curves of a) symmetric gold-gold and b) non-symmetric gold-graphene amine terminated OPE molecular junctions

The respective transmission curves for Au/Au compared with Au/graphene junctions display notably different behaviors. Both sets of curves feature peaks in the electronic transmissions associated to the HOMO (at negative E-E_F energy values) and LUMO (at positive E-E_F) frontier orbital. However, it is notable that for Au/Au junctions the transmission values are unity (T(E)=1), while for the Au/graphene junctions all resonances sit at T(E)<1. This arises from a larger coupling to the Au electrodes compared to the graphene contacts. For the gold-graphene junctions the graphene contacting preserves the "molecular spectrum" due to the weak coupling through van der Waals interactions. This can be further understood following the general expression of the electronic transmission:

$$T(E_F) = 4\Gamma_L\Gamma_R/[(E_{LUMO}-E_F)^2+(\Gamma_L+\Gamma_R)^2]$$

where E_{LUMO} is the energy of the LUMO (closest level to the Fermi level through which the transport is mediated), and $\Gamma_{L/R}$ represents the left (right) coupling to the electrodes. In the case of gold-gold junction, when E_{LUMO} is very close to the Fermi level, the term $(E_{LUMO}-E_F)$ becomes negligible and *T(E)* goes to 1, since $\Gamma_L = \Gamma_R$. In the gold-graphene junction however, the situation is a bit more complex, due to different couplings at the gold and graphene interfaces. Also, in that case, the Fermi level lies in the mid-gap and the previous formula should be modified to take into account potential resonances with both HOMO and LUMO. As a result, the electronic transmission will be always lower than 1.

In addition for the Au/Au junctions an important electronic response is clearly observed in the HOMO-LUMO gap, due to this key coupling with the gold electrodes (see Figure 4(a)). Indeed, an important coupling at the molecule-electrode interface is responsible for a widening of the electronic levels, leading to a more important density in the gap. This pronounced bump in the HOMO-LUMO gap of the transmission curve is particular clear for the

shorter molecular bridges (Au/**1a**/Au and Au/**2a**/Au), as seen in the black and red curves of Figure 4(a). In addition, an important shift of the HOMO level toward the Fermi energy, between the symmetric (gold-gold) and asymmetric (gold-graphene) configurations is also clear. For example, the HOMO resonance for Au/**3a**/Au is at about -2.2 eV, while it is much closer to the Fermi level for Au/**3a**/graphene junctions (-1.4 eV). This aspect is very similar to what we have observed in our previous works on alkanedithiol [60] and alkanediamine [42] MJs between gold-gold or gold-graphene electrodes. In both cases, the HOMO level has been shifted significantly closer to the Fermi level due to a symmetry breaking induced by the introduction of the graphene electrode. The key point here lies in the difference of couplings at each interface, namely a covalent coupling at the gold-molecule interface and a van der Waals coupling at the graphene-molecule interface. This is what then leads to the reduction of the attenuation factor. Indeed, within a simple barrier tunneling model, as used in the Simmons model [61], the attenuation factor varies as the square root of the barrier-height at the molecule-electrode interface. Here this barrier may in a simple model be characterized by the energy difference between the Fermi and the HOMO level. As a result, the HOMO shift towards the Fermi level induces a reduction of the attenuation factor. It is interesting to compare with our previous work on phenyl chains, [43] where electronic density was fully localized on the aromatic rings of the molecular bridge, leading to a full electronic decoupling of the molecule from the electrodes. By contrast in our present work with OPE bridges, the presence of triple carbon bonds leads to a delocalization of the electronic density, which couples strongly to the gold electrodes. This result confirms a general trend previously noted that molecular wires featuring aromatic rings linked by acetylene groups (i.e. OPEs) present a better coupling to the electrode, due a more significant electronic delocalization, than oligo-phenyl molecular wires where the electronic density is more localized on the molecular rings [62].

Conductance of methyl sulfide terminated OPE molecules

In order to further confirm the effect of non-symmetric electrode contacting on the length dependence of OPE based molecules, we replaced the amine termination with the methyl sulfide group and measured the conductance of each MJs. The typical conductance traces and the 1D conductance histograms of **1b**-**3b** with Au electrodes are shown in Figure 5(a-d), respectively. The broad Gaussian distribution peak in Figure 5(b) represents the most probable conductance value of 480 nS for Au/**1b**/Au. Our results agree well with the studies reported by Yoo *et al.* and Zhao *et al.* [45, 63] Comparing to the conductance of **1a** with Au electrodes, the molecular junction formed by **1b** with Au electrodes system gives a slightly higher conductance, however within the uncertainty window of measurement the values are comparable. Here it can be noted that these two anchoring groups also have similar binding strengths to gold electrodes, with Venkataraman *et al.* using an AFM to measure the binding forces of amine and methyl sulfide group with gold to be 0.5 nN and 0.7 nN, respectively. [25, 64] As shown in Figure

5 (c-d), the most probable conductance values of Au/**2b**/Au and Au/**3b**/Au MJs are found as 53 nS and 8.2 nS, respectively. The conductance values of MJs formed by methyl sulfide terminated OPE molecules between Au and graphene electrodes were also measured under the same condition. The typical conductance traces and the 1D conductance histograms are shown in Figure 5(e-h). The conductance values of **1b**-**3b** with Au and graphene electrodes are found to be 41 nS, 20 nS and 8.2 nS, respectively. The MJs formed by **1b**-**2b** with Au electrodes show higher conductance values than that formed by **1b**-**2b** with Au and graphene electrodes. However, the conductance values of the Au/**3b**/graphene junction and Au/**3b**/Au junction are essentially identical.

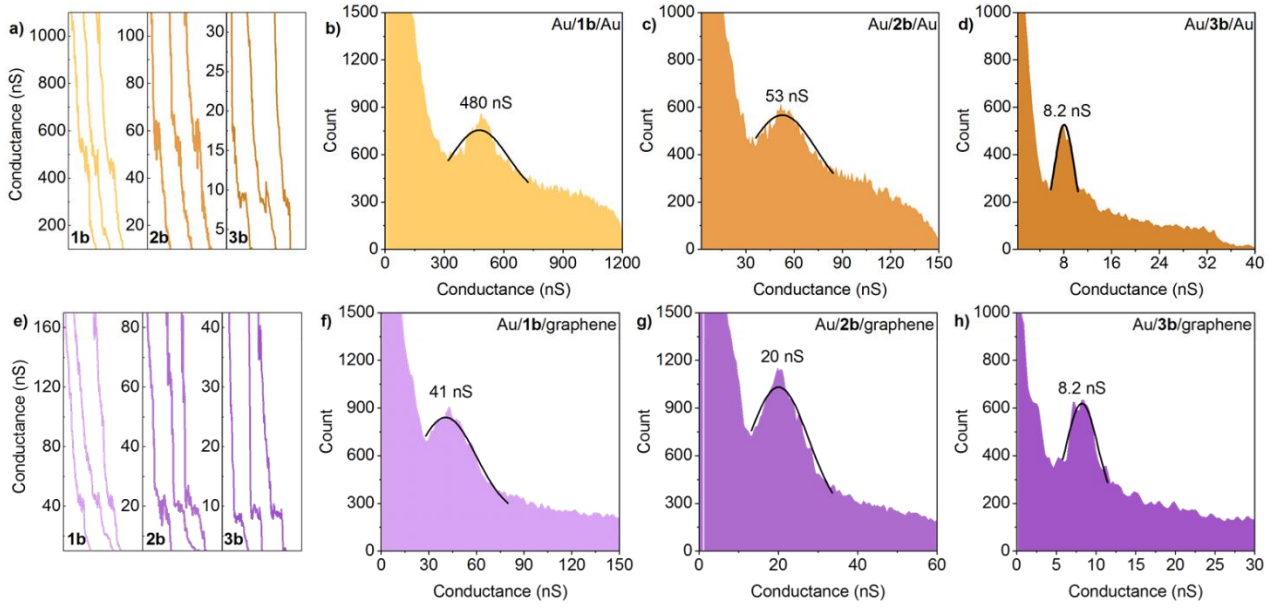

Figure 5. Typical conductance traces of methyl sulfide terminated OPE molecules (a) with Au/Au electrode; (e) with Au/graphene electrode system. 1D conductance histograms of methyl sulfide terminated OPE molecules (b-d); with Au/Au electrode (f-h) with Au/graphene electrode contacting. The black lines represent the Gaussian distribution peak fitting curves of each molecular junctions.

Again, we have studied these MJs theoretically using density functional theory. The corresponding optimized geometries for the model MJs are represented in Figure 6. From these configurations, we have determined the corresponding electronic transmission, which is represented in Figure 7(a) for the gold-gold junctions and in Figure 7(b) for the gold-graphene junctions, respectively.

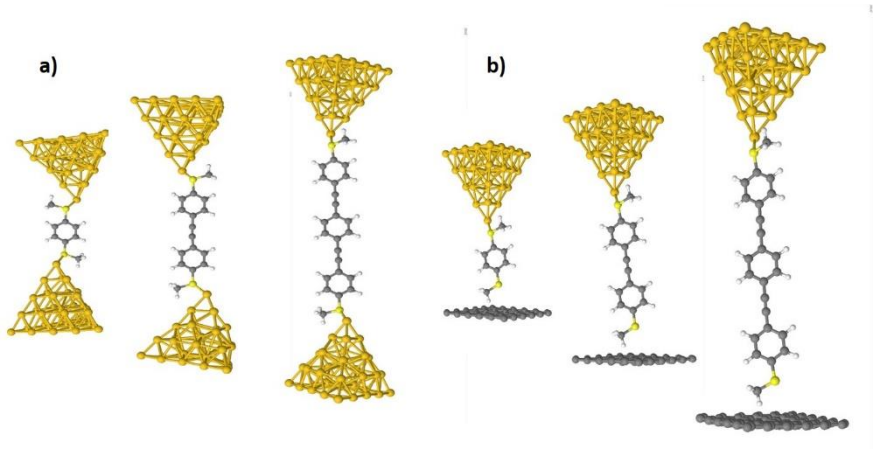

Figure 6. DFT optimized atomic configurations of a) symmetric gold-gold and b) asymmetric gold-graphene methyl sulfide terminated OPE molecular junctions

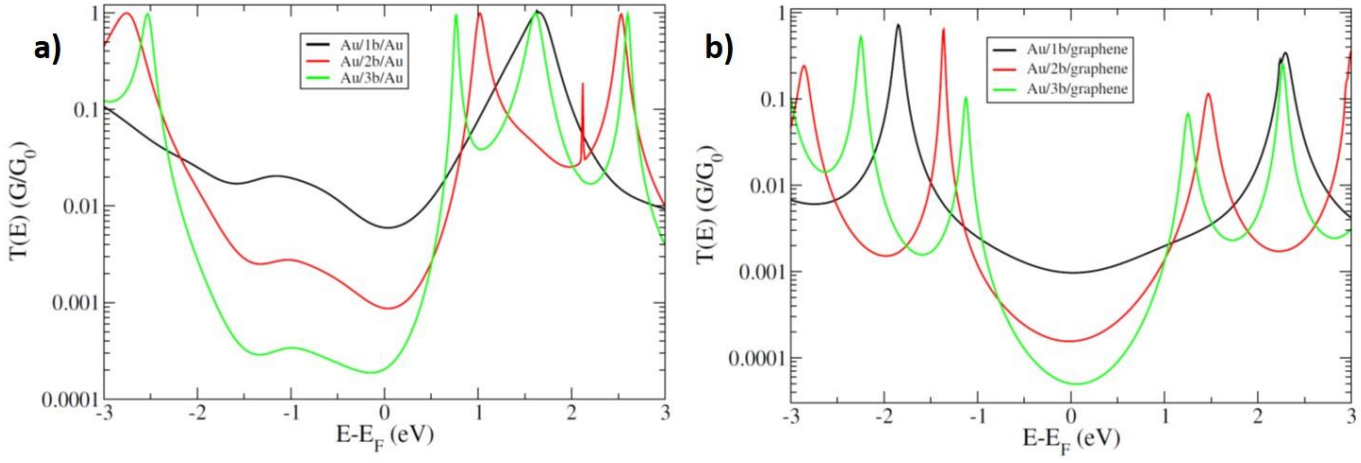

Figure 7. Calculated electronic transmissions of a) symmetric gold-gold and b) non-symmetric gold-graphene methyl sulfide terminated OPE molecular junctions

From these electronic transmissions, we can draw the same general conclusions as for the of amine terminated MJs. As is often the case in molecular electronics, the general electronic behavior is broadly similar in symmetric junctions, independently of the anchoring groups, as can be observed here. For non-symmetric junction contacting, the electronic transport properties are modified but in the same way for different anchoring groups, but the modification is attributed predominantly to the change of electrode type. Note that when comparing the amine (Figure 4(a)) with the methyl sulfide (Figure 7(a)) anchored gold-molecule-gold junctions, the transmission curves are shifted further toward negative energies for the methyl sulfide anchored junctions. For the methyl sulfide anchored junctions this yields a non-resonant tunneling regime which is then dominated by the LUMO orbital (Figure 7(a)), i.e. the transport of electrons. With the symmetry breaking induced by the graphene electrode, the

whole transmission spectrum shifts to the right (Figure 7(b)) leading to the Fermi level being placed rather centrally between the HOMO and LUMO levels.

Break-off distances of the junctions

Figure 8 (a) shows a 2D distance-conductance histogram of Au/**3a**/Au junctions. The possible conductance range of the Au/**3a**/Au junction (8.2 nS- 17 nS) is marked in the upper red area of the histogram by the green dotted boundary lines. The lower red area, at conductance values < 5 nS, corresponds to the break-off decay after the molecular junction breaks. The break-off distance ($S_{break\text{-}off}$) of each MJs is calculated by using a modified published method. [65] For a molecular junction measured by using STM-*I(s)* technique, $S_{break\text{-}off}$ is the sum of the initial set point distance (S_0) of the Au STM tip plus the distance at which the junction breaks upon piezo retraction obtained from experiments (S_w). $S_{break\text{-}off}$ then quantifies the most probable stretching length of the molecular junction when it breaks upon piezo retraction. The initial set point distance (S_0) can be varied by adjusting the set point current (I_0). The value of S_0 is usually estimated by measuring the current decay in the empty tunneling gap and then using a calculation which involves the conductance which would correspond to point contact between the tip and substrate. This procedure is detailed in the literature. Briefly, when no molecular junction is formed, the conductance value of tip-substrate gap is known to decrease approximately exponentially with increasing gap distance. Therefore, the natural logarithm of the current ($\ln I$) varies linearly with the tip-substrate gap distance.This slope ($d\ln I/ds$) is obtained by linear regression and then S_0 can be estimated by extrapolating the current from the set point to the tip-substrate point contact. S_w is obtained by statistically analyzing the distance displaced by the STM tip from the set point current starting distance to the molecular junction breaking distance. Figure 8(b) shows the 1D stretching distance histogram of the distance (S_w) measured in the experiments with Au/**3a**/Au junctions. The value of S_w is found as 0.75 ± 0.26 nm by Gaussian distribution peak fitting of this 1D distance histogram. Table 1 summarizes the molecular lengths and $S_{break\text{-}off}$ of all the molecules studied in this work. Details of calculation for $S_{break\text{-}off}$ can be found in supporting information. In most cases, the molecule is not fully stretched when the MJs were broken. This is reflected by the break-off distance of the molecular junction being smaller than the length of the molecule itself. For short molecules, the break-off distance is comparable to the molecular length within uncertainty limits.

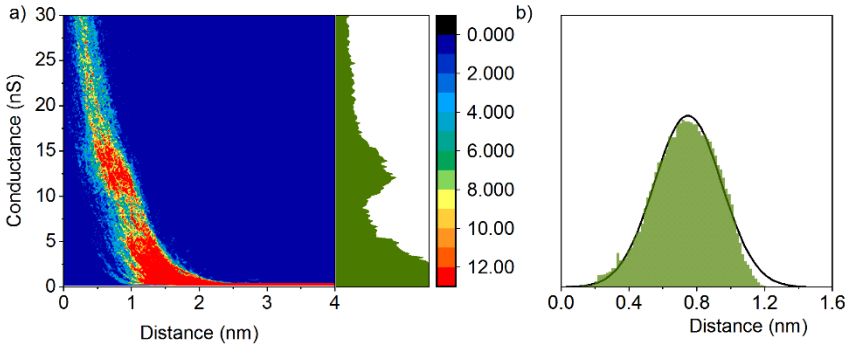

Figure 8 (a) 2D distance-conductance histogram of Au/**3a**/Au junctions; (b) 1D distance histogram of S_w. The black line represents the Gaussian distribution peak fitting curve of S_w.

Table 1. The molecular length and break-off distance of each molecule

Molecule	Molecular length (nm)	Break-off distance (nm)	
		Au-Au	Au-graphene
1a	0.53	0.52±0.12	0.51±0.11
2a	1.19	0.90±0.08	0.93±0.06
3a	1.86	1.64±0.26	1.02±0.11
1b	0.64	0.70±0.08	0.70±0.13
2b	1.30	1.02±0.09	1.03±0.15
3b	1.94	1.74±0.33	1.75±0.27

Attenuation factor of OPE based molecular junctions

From our measurements and calculations, we have determined the attenuation factors of amine and methyl sulfide terminated OPE molecules. The natural logarithm of the conductance vs. molecular length of each molecular junction has been plotted, with the attenuation factors being determined through linear fitting, as shown in Figure 9. Table 2 summarizes the conductance and attenuation factors of the studied molecules with different electrode systems. The β values of the MJs formed by amine and methyl sulfide terminated OPE molecules with Au electrodes are determined as 2.7 nm^{-1} and 3.1 nm^{-1}, respectively, while smaller values of 1.1 nm^{-1} and 1.3 nm^{-1} are found for hybrid Au/graphene electrodes. For both amine and methyl sulfide terminated OPE molecules, the introduction of graphene electrode leads a noticeable decrease of attenuation factors. As indicated in the Conductance of amine terminated OPE molecules section, through the analysis of the molecular levels and the use of the Simmons' model, this reduction can be attributed to the shift of the molecular levels with

the introduction of the graphene electrode, similarly to what occurs for alkanedithiol [60] and alkanediamine [42] MJs under the same conditions. Consequently, we can deduce that the combination of aromatic phenyl rings with interconnecting acetylene linkers in the OPE chain results in the electronic density being delocalized effectively along the while MJs. This behavior is very similar to that for alkane chains and opposite to the behavior of phenyl chains. This feature is very interesting since alkane chains present a σ-like electronic conduction[47] while phenyl and OPE chains present a π-like electronic conduction[27]. In this respect, the attenuation factor can be reduced by using a graphene electrode, leading to a higher conductance than would otherwise be the case for longer molecular chains.

This work also reveals that there is not much difference in the electrical properties of amine and methyl sulfide terminated MJs. Both the attenuation factor, as expected, but also more surprisingly on the conductance have similar values. This latter observation is corroborated by the determination of contact resistance of the MJs, which is the pre-factor of the exponential in the conductance evolution. By extending the fit of experimental data of Figure 9 to zero length, the contact resistance is estimated as 0.53 MΩ and 10 MΩ for amine terminated Au/Au and Au/graphene MJs, while for methyl sulfide terminated Au/Au and Au/graphene MJs values of 0.30 MΩ and 10 MΩ are respectively obtained. The observed higher contact resistance for Au/graphene electrodes with respect to Au electrodes is consistent with our previous studies.[47] Zhang and co-workers reported that introducing graphene electrode can change the contact resistance to 3.9 MΩ for Au/*n*-alkanedithiol/graphene junctions, which is significantly higher than for Au symmetric contacts (27 kΩ).

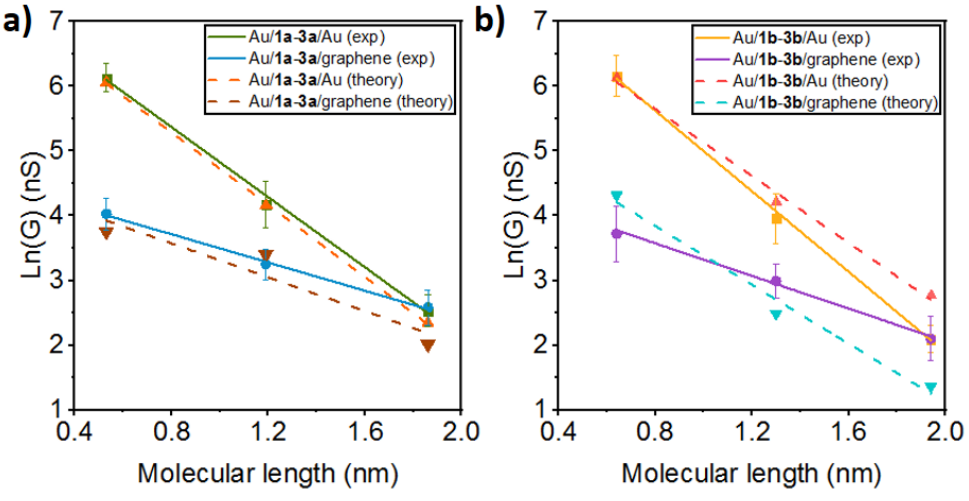

Figure 9. Natural logarithmic plots of the conductance as a function of the molecular length for a) amine and b) methyl sulfide terminated MJs. The lines represent the linear fitting for each molecular junction.

Table 2. Conductance and attenuation factors of **1a**-**3a** and **1b**-**3b** with Au/Au and Au/graphene electrode system

Molecule	Conductance (nS)		Attenuation factors (nm^{-1})		Contact resistance (MΩ)	
	Experiment	Theory	Experiment	Theory	Experiment	Theory
Au/**1a**/Au	460	430				
Au/**2a**/Au	65	64	2.7	2.8	0.53	0.54
Au/**3a**/Au	13	10				
Au/**1b**/Au	480	460				
Au/**2b**/Au	53	68	3.1	2.6	0.30	0.44
Au/**3b**/Au	8.2	16				
Au/**1a**/graphene	56	43				
Au/**2a**/graphene	26	30	1.1	1.3	10	9.8
Au/**3a**/graphene	13	7.5				
Au/**1b**/graphene	41	75				
Au/**2b**/graphene	20	12	1.3	2.3	10	3.4
Au/**3b**/graphene	8.2	3.9				

Conclusions

In summary, we have systematically studied the effect of anti-symmetric (or asymmetric) connecting on the conductance and length dependence of OPE based MJs using Au/Au or Au/graphene electrodes. The conductance and attenuation factor of amine and methyl sulfide terminated OPE molecules have been determined experimentally and theoretically. Both amine and methyl sulfide terminated MJs present similar conductance values and attenuation factors. For Au/graphene MJs, both systems present lower attenuation factor than that of analogous Au contact pairs. This is attributed to a shift of the molecular levels closer to the Fermi level, which reduces the electronic potential barrier at the interface and consequently the attenuation factor. Also, a lower conductance is observed for OPE based molecular junction with Au and graphene electrodes, which is associated to the relatively weak coupling at the molecule-graphene electrode interface. In that respect, the OPE based MJs present an electronic behavior similar to that of alkane based molecular chains. In the OPE MJs the acetylene groups linking adjacent phenyl groups promote a good electronic conjugation across the molecular bridge, which

is in contrast to oligo-phenyl MJs where the electronic density is localized, which causes the influence of electrodes or anchoring groups to be reduced. Finally, this work confirms that for the delocalized electronic system, the symmetry breaking induced by the graphene electrode helps in enhancing the electronic transport properties of the molecular junctions.

Conflict of interest

The authors declare no competing financial interest.

Supporting Information

The synthesis procedures of **1b**, **2b**, **3b**, 2D distance-conductance histograms, calculation of break-off distance, *I-V* curves are supplied as Supporting Information.

Acknowledgment

This work was supported by the National Natural Science Foundation of China (NSFC Grants 21750110441, 21503169), Suzhou Industrial Park Initiative Platform Development for Suzhou Municipal Key Lab for New Energy Technology (RR0140), Key Program Special Fund in XJTLU (KSF-A-04 and KSF-A-07) and the XJTLU Research Development Fund (PGRS-13-01-03, RDF-14-02-42 and RDF-16-01-33).

References

1. Aviram, A.; Ratner, M. A., Molecular Rectifiers. *Chem. Phys. Lett.* **1974**, *29*, 277-283.
2. Wada, Y., A Prospect for Single Molecule Information Processing Devices. *Pure Appl Chem* **1999**, *71*, 2055-2066.
3. Beckman, R.; Beverly, K.; Boukai, A.; Bunimovich, Y.; Choi, J. W.; DeIonno, E.; Green, J.; Johnston-Halperin, E.; Luo, Y.; Sheriff, B., et al., Spiers Memorial Lecture. Molecular Mechanics and Molecular Electronics. *Faraday Discuss.* **2006**, *131*, 9-22.
4. Wang, K., DNA-Based Single-Molecule Electronics: From Concept to Function. *J. Funct. Biomater.* **2018**, *9*, 8/1-8/31.
5. Liu, J.; Huang, X.; Wang, F.; Hong, W., Quantum Interference Effects in Charge Transport through Single-Molecule Junctions: Detection, Manipulation, and Application. *Acc. Chem. Res.* **2019**, *52*, 151-160.
6. Bergren, A. J.; Zeer-Wanklyn, L.; Semple, M.; Pekas, N.; Szeto, B.; McCreery, R. L., Musical Molecules: The Molecular Junction as an Active Component in Audio Distortion Circuits. *J. Phys.: Condens. Matter* **2016**, *28*, 094011/1-094011/11.

7. Roldan, D.; Kaliginedi, V.; Cobo, S.; Kolivoska, V.; Bucher, C.; Hong, W.; Royal, G.; Wandlowski, T., Charge Transport in Photoswitchable Dimethyldihydropyrene-Type Single-Molecule Junctions. *J. Am. Chem. Soc.* **2013**, *135*, 5974-5977.
8. Kim, T.; Liu, Z. F.; Lee, C.; Neaton, J. B.; Venkataraman, L., Charge Transport and Rectification in Molecular Junctions Formed with Carbon-Based Electrodes. *Proc. Natl. Acad. Sci. U. S. A.* **2014**, *111*, 10928-10932.
9. Horiguchi, K.; Sagisaka, T.; Kurokawa, S.; Sakai, A., Electron Transport through Ni/1,4-Benzenedithiol/Ni Single-Molecule Junctions under Magnetic Field. *J. Appl. Phys. (Melville, NY, U. S.)* **2013**, *113,* 144313/1-144313/7.
10. Nitzan, A.; Ratner, M. A., Electron Transport in Molecular Wire Junctions. *Science (Washington, DC, U. S.)* **2003**, *300*, 1384-1389.
11. Matthews, N.; Hagmann, M. J.; Mayer, A., Comment: "Generalized Formula for the Electric Tunnel Effect between Similar Electrodes Separated by a Thin Insulating Film" [J. Appl. Phys. 34, 1793 (1963)]. *J. Appl. Phys. (Melville, NY, U. S.)***2018**, *123*, 136101/1.
12. Nitzan, A., Electron Transmission through Molecules and Molecular Interfaces. *Annu. Rev. Phys. Chem.***2001,** *52*, 681-750.
13. Chen, F.; Li, X.; Hihath, J.; Huang, Z.; Tao, N., Effect of Anchoring Groups on Single-Molecule Conductance: Comparative Study of Thiol-, Amine-, and Carboxylic-Acid-Terminated Molecules. *J. Am. Chem. Soc.* **2006**, *128*, 15874-15881.
14. Moreno-Garcia, P.; Gulcur, M.; Manrique, D. Z.; Pope, T.; Hong, W.; Kaliginedi, V.; Huang, C.; Batsanov, A. S.; Bryce, M. R.; Lambert, C., et al., Single-Molecule Conductance of Functionalized Oligoynes: Length Dependence and Junction Evolution. *J. Am. Chem. Soc.* **2013**, *135*, 12228-12240.
15. Park, S.; Kang, S.; Yoon, H. J., Power Factor of One Molecule Thick Films and Length Dependence. *ACS Cent. Sci.* **2019**, *5*, 1975-1982.
16. Huang, C.; Rudnev, A. V.; Hong, W.; Wandlowski, T., Break Junction under Electrochemical Gating: Testbed for Single-Molecule Electronics. *Chem. Soc. Rev.* **2015**, *44*, 889-901.
17. Su, T. A.; Neupane, M.; Steigerwald, M. L.; Venkataraman, L.; Nuckolls, C., Chemical Principles of Single-Molecule Electronics. *Nat. Rev. Mater* **2016**, *1,* 16002/1-16002/15.
18. Akkerman, H. B.; de Boer, B., Electrical Conduction through Single Molecules and Self-Assembled Monolayers. *J. Phys.: Condens. Matter* **2007**, *20*, 013001/1-013001/20.
19. Busiakiewicz, A.; Karthäuser, S.; Homberger, M.; Kowalzik, P.; Waser, R.; Simon, U., Electronic Transport Properties of Individual 4,4' -Bis(Mercaptoalkyl)-Biphenyl Derivatives Measured in Stm-Based Break Junctions. *Phys. Chem. Chem. Phys.* **2010**, *12*, 10518-10524.
20. Venkataraman, L.; Klare, J. E.; Nuckolls, C.; Hybertsen, M. S.; Steigerwald, M. L., Dependence of Single-Molecule Junction Conductance on Molecular Conformation. *Nature (London, U. K.)* **2006**, *442*, 904-907.
21. He, J.; Chen, F.; Li, J.; Sankey, O. F.; Terazono, Y.; Herrero, C.; Gust, D.; Moore, T. A.; Moore, A. L.; Lindsay, S. M., Electronic Decay Constant of Carotenoid Polyenes from Single-Molecule Measurements. *J. Am. Chem. Soc.* **2005**, *127*, 1384-1385.
22. Wang, C.; Batsanov, A. S.; Bryce, M. R.; Martín, S.; Nichols, R. J.; Higgins, S. J.; García-Suárez, V. M.; Lambert, C. J., Oligoyne Single Molecule Wires. *J. Am. Chem. Soc.* **2009**, *131*, 15647-15654.
23. Kaliginedi, V.; Rudnev, A. V.; Moreno-Garcia, P.; Baghernejad, M.; Huang, C.; Hong, W.; Wandlowski, T., Promising Anchoring Groups for Single-Molecule Conductance Measurements. *Phys. Chem. Chem. Phys.* **2014**, *16*, 23529-23539.
24. Hihath, J.; Tao, N., The Role of Molecule–Electrode Contact in Single-Molecule Electronics. *Semicond. Sci. Technol.* **2014**, *29,* 054007/1-054007/8.
25. Park, Y. S.; Whalley, A. C.; Kamenetska, M.; Steigerwald, M. L.; Hybertsen, M. S.; Nuckolls, C.; Venkataraman, L., Contact Chemistry and Single-Molecule Conductance: A Comparison of Phosphines, Methyl Sulfides, and Amines. *J. Am. Chem. Soc.* **2007**, *129*, 15768-15769.
26. Venkataraman, L.; Klare, J. E.; Tam, I. W.; Nuckolls, C.; Hybertsen, M. S.; Steigerwald, M. L., Single-Molecule Circuits with Well-Defined Molecular Conductance. *Nano Lett.* **2006**, *6*, 458-462.

27. Tao, S.; Zhang, Q.; He, C.; Lin, X.; Xie, R.; Zhao, C.; Zhao, C.; Smogunov, A.; Dappe, Y. J.; Nichols, R. J., et al., Graphene-Contacted Single Molecular Junctions with Conjugated Molecular Wires. *ACS Appl. Nano Mater.* **2018**, *2*, 12-18.
28. Ozawa, H., et al., Synthesis and Single-Molecule Conductance Study of Redox-Active Ruthenium Complexes with Pyridyl and Dihydrobenzo[b]Thiophene Anchoring Groups. *Chem. - Eur. J.* **2016**, *22*, 12732-12740.
29. Zhao, X.; Huang, C.; Gulcur, M.; Batsanov, A. S.; Baghernejad, M.; Hong, W.; Bryce, M. R.; Wandlowski, T., Oligo(Aryleneethynylene)s with Terminal Pyridyl Groups: Synthesis and Length Dependence of the Tunneling-to-Hopping Transition of Single-Molecule Conductances. *Chem. Mater.* **2013**, *25*, 4340-4347.
30. He, C.; Zhang, Q.; Fan, Y.; Zhao, C.; Zhao, C.; Ye, J.; Dappe, Y. J.; Nichols, R. J.; Yang, L., Effect of Asymmetric Anchoring Groups on Electronic Transport in Hybrid Metal/Molecule/Graphene Single Molecule Junctions. *ChemPhysChem* **2019**, *20*, 1830-1836.
31. Li, J.; Chen, Z.; Wang, Y.; Zhou, X.; Xie, L.; Shi, Z.; Liu, J.; Yan, J.; Mao, B., Single-Molecule Anisotropic Magnetoresistance at Room Temperature: Influence of Molecular Structure. *Electrochim. Acta* **2021**, *389*, 138760/1-138760/8.
32. Capozzi, B.; Dell, E. J.; Berkelbach, T. C.; Reichman, D. R.; Venkataraman, L.; Campos, L. M., Length-Dependent Conductance of Oligothiophenes. *J. Am. Chem. Soc.* **2014**, *136*, 10486-10492.
33. Kim; Beebe, J. M.; Jun, Y.; Zhu, X. Y.; Frisbie, C. D., Correlation between Homo Alignment and Contact Resistance in Molecular Junctions: Aromatic Thiols Versus Aromatic Isocyanides. *J. Am. Chem. Soc.* **2006**, *128*, 4970-4971.
34. Hong, W.; Li, H.; Liu, S. X.; Fu, Y.; Li, J.; Kaliginedi, V.; Decurtins, S.; Wandlowski, T., Trimethylsilyl-Terminated Oligo(Phenylene Ethynylene)s: An Approach to Single-Molecule Junctions with Covalent Au-C Sigma-Bonds. *J. Am. Chem. Soc.* **2012**, *134*, 19425-19431.
35. Gunasekaran, S.; Hernangómez-Pérez, D.; Davydenko, I.; Marder, S.; Evers, F.; Venkataraman, L., Near Length-Independent Conductance in Polymethine Molecular Wires. *Nano Lett.* **2018**, *18*, 6387-6391.
36. Choi, B.; Capozzi, B.; Ahn, S.; Turkiewicz, A.; Lovat, G.; Nuckolls, C.; Steigerwald, M. L.; Venkataraman, L.; Roy, X., Solvent-Dependent Conductance Decay Constants in Single Cluster Junctions. *Chem. Sci.* **2016**, *7*, 2701-2705.
37. Milan, D. C.; Al-Owaedi, O. A.; Oerthel, M.-C.; Marqués-González, S.; Brooke, R. J.; Bryce, M. R.; Cea, P.; Ferrer, J.; Higgins, S. J.; Lambert, C. J., et al., Solvent Dependence of the Single Molecule Conductance of Oligoyne-Based Molecular Wires. *J. Phys. Chem. C* **2015**, *120*, 15666-15674.
38. Xie, Z.; Baldea, I.; Frisbie, C. D., Energy Level Alignment in Molecular Tunnel Junctions by Transport and Spectroscopy: Self-Consistency for the Case of Alkyl Thiols and Dithiols on Ag, Au, and Pt Electrodes. *J. Am. Chem. Soc.* **2019**, *141*, 18182-18192.
39. Liu, L.; Zhang, Q.; Tao, S.; Zhao, C.; Almutib, E.; Al-Galiby, Q.; Bailey, S. W.; Grace, I.; Lambert, C. J.; Du, J., et al., Charge Transport through Dicarboxylic-Acid-Terminated Alkanes Bound to Graphene-Gold Nanogap Electrodes. *Nanoscale* **2016**, *8*, 14507-14513.
40. Adak, O.; Kladnik, G.; Bavdek, G.; Cossaro, A.; Morgante, A.; Cvetko, D.; Venkataraman, L., Ultrafast Bidirectional Charge Transport and Electron Decoherence at Molecule/Surface Interfaces: A Comparison of Gold, Graphene, and Graphene Nanoribbon Surfaces. *Nano Lett.* **2015**, *15*, 8316-8321.
41. Li, H.; Su, T. A.; Camarasa-Gomez, M.; Hernangomez-Perez, D.; Henn, S. E.; Pokorny, V.; Caniglia, C. D.; Inkpen, M. S.; Korytar, R.; Steigerwald, M. L., et al., Silver Makes Better Electrical Contacts to Thiol-Terminated Silanes Than Gold. *Angew. Chem., Int. Ed.* **2017**, *56*, 14145-14148.
42. Zhou, X. Y.; Peng, Z. L.; Sun, Y. Y.; Wang, L. N.; Niu, Z. J.; Zhou, X. S., Conductance Measurement of Pyridyl-Based Single Molecule Junctions with Cu and Au Contacts. *Nanotechnology* **2013**, *24*, 465204/1-465204/9.
43. Planje, I. J.; Davidson, R. J.; Vezzoli, A.; Daaoub, A.; Sangtarash, S.; Sadeghi, H.; Martin, S.; Cea, P.; Lambert, C. J.; Beeby, A., et al., Selective Anchoring Groups for Molecular Electronic Junctions with Ito Electrodes. *ACS Sens.* **2021**, *6*, 530-537.

44. Cao, Y.; Dong, S.; Liu, S.; He, L.; Gan, L.; Yu, X.; Steigerwald, M. L.; Wu, X.; Liu, Z.; Guo, X., Building High-Throughput Molecular Junctions Using Indented Graphene Point Contacts. *Angew. Chem., Int. Ed.* **2012**, *51*, 12228-12232.
45. Yoo, P. S.; Kim, T., Linker-Dependent Junction Formation Probability in Single-Molecule Junctions. *Bull. Korean Chem. Soc.* **2015**, *36*, 265-268.
46. He, C.; Zhang, Q.; Tao, S.; Zhao, C.; Zhao, C.; Su, W.; Dappe, Y. J.; Nichols, R. J.; Yang, L., Carbon-Contacted Single Molecule Electrical Junctions. *Phys. Chem. Chem. Phys.* **2018**, *20*, 24553-24560.
47. Zhang, Q.; Tao, S.; Yi, R.; He, C.; Zhao, C.; Su, W.; Smogunov, A.; Dappe, Y. J.; Nichols, R. J.; Yang, L., Symmetry Effects on Attenuation Factors in Graphene-Based Molecular Junctions. *J. Phys. Chem. Lett.***2017**, *8*, 5987-5992.
48. Wang, L. J.; Yong, A.; Zhou, K. G.; Tan, L.; Ye, J.; Wu, G. P.; Xu, Z. G.; Zhang, H. L., Conformation-Controlled Electron Transport in Single-Molecule Junctions Containing Oligo(Phenylene Ethynylene) Derivatives. *Chem. - Asian J.* **2013**, *8*, 1901-1909.
49. Huber, R.; González, M. T.; Wu, S.; Langer, M.; Grunder, S.; Horhoiu, V.; Mayor, M.; Bryce, M. R.; Wang, C.; Jitchati, R., et al., Electrical Conductance of Conjugated Oligomers at the Single Molecule Level. *J. Am. Chem. Soc.* **2008**, *130*, 1080-1084.
50. Kaliginedi, V.; Moreno-Garcia, P.; Valkenier, H.; Hong, W.; Garcia-Suarez, V. M.; Buiter, P.; Otten, J. L.; Hummelen, J. C.; Lambert, C. J.; Wandlowski, T., Correlations between Molecular Structure and Single-Junction Conductance: A Case Study with Oligo(Phenylene-Ethynylene)-Type Wires. *J. Am. Chem. Soc.***2012**, *134*, 5262-5275.
51. O'Driscoll, L. J.; Bryce, M. R., A Review of Oligo(Arylene Ethynylene) Derivatives in Molecular Junctions. *Nanoscale* **2021**, *13*, 10668-10711.
52. Joseph, P. J. A.; Priyadarshini, S.; Kantam, M. L.; Sreedhar, B., Investigation of the Scope and Mechanism of Copper Catalyzed Regioselective Methylthiolation of Aryl Halides. *Tetrahedron* **2013**, *69*, 8276-8283.
53. Haiss, W.; van Zalinge, H.; Higgins, S. J.; Bethell, D.; Höbenreich, H.; Schiffrin, D. J.; Nichols, R. J., Redox State Dependence of Single Molecule Conductivity. *J. Am. Chem. Soc.* **2003**, *125*, 15294-15295.
54. Ren, B.; Picardi, G.; Pettinger, B., Preparation of Gold Tips Suitable for Tip-Enhanced Raman Spectroscopy and Light Emission by Electrochemical Etching. *Rev. Sci. Instrum.* **2004**, *75*, 837-841.
55. Zhang, Q.; Liu, C.; Tao, S.; Yi, R.; Su, W.; Zhao, C.; Zhao, C.; Dappe, Y. J.; Nichols, R. J.; Yang, L., Fast and Straightforward Analysis Approach of Charge Transport Data in Single Molecule Junctions. *Nanotechnology* **2018**, *29*, 325701/1-325701/9.
56. Lewis, J. P.; Jelínek, P.; Ortega, J.; Demkov, A. A.; Trabada, D. G.; Haycock, B.; Wang, H.; Adams, G.; Tomfohr, J. K.; Abad, E., et al., Advances and Applications in the FIREBALL ab Initio Tight-Binding Molecular-Dynamics Formalism. *Phys. Status Solidi B* **2011,** *248*, 1989-2007.
57. Pitié, S.; Seydou, M.; Dappe, Y. J.; Martin, P.; Lacroix, J. C., Insights on asymmetric BTB-Based Molecular Junctions: effects of electrode coupling. *Chemical Physics Letters* **2021**, DOI:10.1016/j.cplett.2021.139273.
58. Zhao, Z.; Liu, R.; Mayer, D.; Coppola, M.; Sun, L.; Kim, Y.; Wang, C.; Ni, L.; Chen, X.; Wang, M., et al., Shaping the Atomic-Scale Geometries of Electrodes to Control Optical and Electrical Performance of Molecular Devices. *Small* **2018**, *14*, 1703815/1-1703815/9.
59. Hong, W.; Manrique, D. Z.; Moreno-Garcia, P.; Gulcur, M.; Mishchenko, A.; Lambert, C. J.; Bryce, M. R.; Wandlowski, T., Single Molecular Conductance of Tolanes: Experimental and Theoretical Study on the Junction Evolution Dependent on the Anchoring Group. *J. Am. Chem. Soc.* **2012**, *134*, 2292-2304.
60. Zhang, Q.; Liu, L.; Tao, S.; Wang, C.; Zhao, C.; Gonzalez, C.; Dappe, Y. J.; Nichols, R. J.; Yang, L., Graphene as a Promising Electrode for Low-Current Attenuation in Nonsymmetric Molecular Junctions. *Nano Lett.* **2016**, *16*, 6534-6540.
61. Simmons, J. G., Generalized Formula for the Electric Tunnel Effect between Similar Electrodes Separated by a Thin Insulating Film. *J. Appl. Phys. (Melville, NY, U. S.)* **1963**, *34*, 1793-1803.
62. Dappe, Y., Attenuation Factors in Molecular Electronics: Some Theoretical Concepts. *Appl. Sci.* **2020**, *10*, 6162/1-6162/8.

63. Zhan, C.; Wang, G.; Zhang, X.-G.; Li, Z.-H.; Wei, J.-Y.; Si, Y.; Yang, Y.; Hong, W.; Tian, Z., Single-Molecule Measurement of Adsorption Free Energy at the Solid–Liquid Interface. *Angew. Chem., Int. Ed.* **2019**, *58*, 14534-14538.
64. Frei, M.; Aradhya, S. V.; Hybertsen, M. S.; Venkataraman, L., Linker Dependent Bond Rupture Force Measurements in Single-Molecule Junctions. *J. Am. Chem. Soc.***2012**, *134*, 4003-4006.
65. Martín, S.; Haiss, W.; Higgins, S.; Cea, P.; López, M. C.; Nichols, R. J., A Comprehensive Study of the Single Molecule Conductance of α, ω-Dicarboxylic Acid-Terminated Alkanes. *J. Phys. Chem. C* **2008**, *112*, 3941-3948.